Carbide Addition on Aluminum Alloy Surface by Plasma Transferred Arc Welding Process†

Fukuhisa MATSUDA*, Kazuhiro NAKATA**, Shigeki SHIMIZU***
and Kensuke NAGAI****

Abstract

Effect of carbide addition on the surface characteristics of aluminum alloy 5083 has been investigated by using the plasma transferred arc welding process with NbC, TiC or SiC powders. Optimum overlaying conditions with good bead appearance and less porosities in overlaid metal were affected with welding current, powder feeding rate and pre-heating temperature of base metal. The maximum area ratio of carbide injected in overlaid metal was about 40% for NbC, TiC, and about 30% for SiC. Hardness increase of overlaid metal by carbide addition was not so large, that is, in the range between Hv 110 and 140. However, abrasive resistance of overlaid metal at higher sliding speed was remarkably improved by the addition of carbide, though at lower sliding speed it was not almost improved. No peeling of overlaid metal from the base metal was observed through bending test.

KEY WORDS: (Metal matrix composite) (Aluminum alloy) (Carbide) (Plasma arc welding) (Hardness) (Wear) (Abrasive resistance)

1. Introduction

Aluminum alloys are widely used as structural materials for various types of equipments and structures for the weight saving. However, higher function or multi-function are required to aluminum alloy component according as the functions of these industrial products become higher. The major drawback of aluminum alloy is its low wear resistance. For this purpose, some methods have been used in practice, such as anodized Al_2O_3, electrolitic hard Cr and ion-plated hard ceramic coating layers. Thicknesses of them are, however, very thin in the order of several μm to several ten μm. Therefore, recently, the establishment of the technology to form thick layer in the order of milli-meter with the superior anti-wear resistance of the surface of aluminum alloy is being strongly required in general. In order to get such a thick layer, surface melting and alloying method by using fusion welding process has been recommended[1] recently. Among fusion welding processes, GTA, GMA, electron beam and laser beam welding processes have been already reported[1-5]. However, plasma arc welding process was not tried yet for this purpose.

In this study, therefore, the plasma transferred arc welding process was employed to form the thick layer superior in wear resistance on the surface of aluminum alloy by adding NbC, TiC and SiC powders and the ranges of optimum welding condition as well as various characteristics of overlaid metal with carbide dispersion was investigated.

2. Materials Used and Experimental Procedures

2.1 Materials used

As a base metal, the aluminum alloy 5083 of 50 mm in thickness was used. Its chemical composition was shown in **Table 1**. As overlaying materials, NbC or TiC powders of 61–147 μm and SiC powder of 88–246 μm in particle size were used.

Table 1 Chemical composition of 5083 aluminum alloy used as base metal (wt%)

Si	Fe	Cu	Mn	Mg	Cr	Zn	Ti	Al
0.35	0.23	0.09	0.47	4.15	0.16	0.19	0.01	Bal.

2.2 Experimental procedures

Applying the powder of NbC, TiC or SiC the bead overlaying test was carried out by plasma transferred arc welding process with a direct current and straight polarity as shown in **Fig. 1** by changing preheating
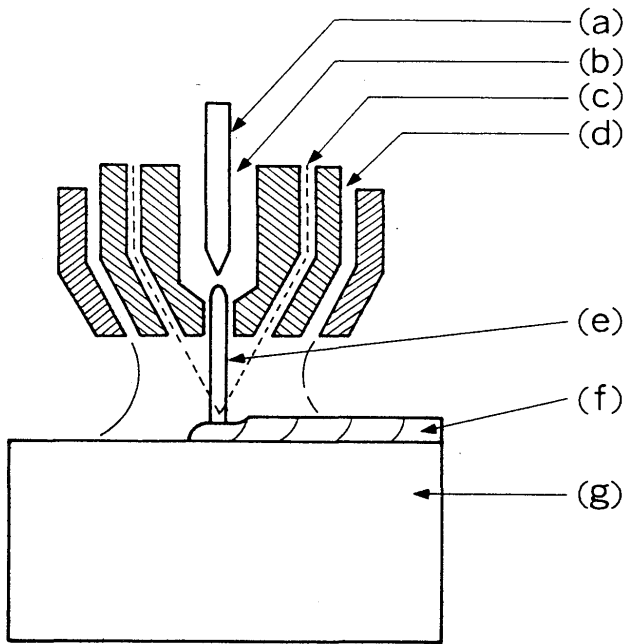
Fig. 1 Principle diagram of plasma transferred arc welding process. (a) Tungsten electrode (cathode), (b) Plasma gas, (c) Powder and powder feeder gas, (d) Shielding gas, (e) Plasma arc, (f) Overlaid metal, (g) Base metal.

temperature, powder feeding rate and welding current. To preheat the base metal, it was heated entirely in an electric furnace up to 400°C. At first, bead appearance test was carried out to check the bead shape and defect. Then, by macrostructural test on the cross-section of the bead, penetration condition was investigated. The cross-sectional area of the bead was measured to obtain the penetration ratio. Further, the cross-section of the bead was observed by a optical microscope and the carbide area ratio in a overlied metal was measured by

the point counting method[5], and the number of porosity if occurred in overlaid metal was also measured. According to these tests results, the range of optimum welding condition was established. Utilizing a welding condition selected from the range of the optimum welding condition, the overlaid metal was prepared on a plate of aluminum alloy by a weaving bead of 50 mm in width with the single or the double layer weldings. Microscopic observation, hardness measurement, wear test and bending test of the overlaid metal were carried out. For the wear test, Ogoshi's Quick Wear Tester was used employing carbon steel (JIS S45C, Hv 234) as an objective material.

3. Experimental Results and Discussion

3.1 Optimum welding condition

3.1.1 Effect of welding condition to bead formation

For each welding current, an excess amount of supplied powder did not form the molten pool on the plate surface, where overlaying welding was impossible as the powder was scattered. Meanwhile, a less amount made the bead appearance inferior. To obtain a good bead appearance, powder feeding rate should be increased as the increases of the welding current and preheating temperature. Weldable range was enlarged as the preheating temperature was increased. **Figure 2** shows the comparison of the ranges of the optimum welding condition in which a good bead appearance was obtained. The range of NbC was the widest and that of TiC was comparably wide, but for SiC the range was considerably narrower than the former two. It
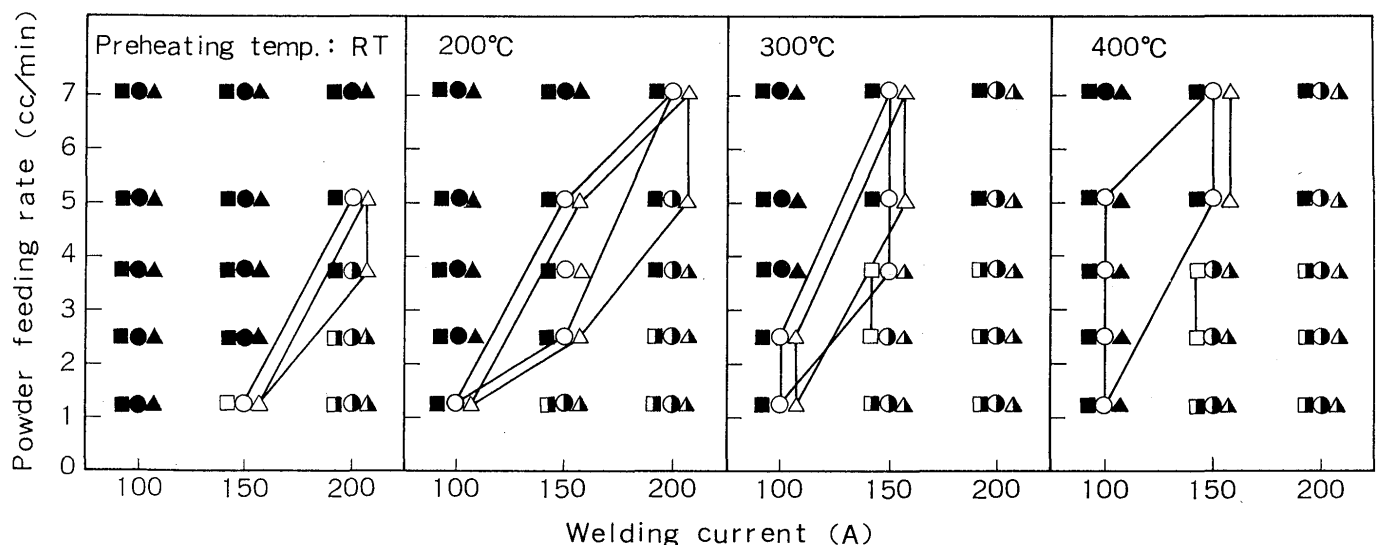

Fig. 2 Comparison of good bead appearance ranges between NbC, TiC and SiC powders.
○ NbC, △ TiC, □ SiC show good bead appearance;
● NbC, ▲ TiC, ■ SiC, weld impossible;
◑ NbC, ▲ TiC, ▣ SiC, irregular bead appearance.

can be assumed that these differences in optimum range are related to the specific weight of carbide, because in the case of low specific weight, the powders feed are likely to be scattered and then gas shieldability of molten metal is decreased, and bead appearance is made poor. Further, on NbC and TiC, the range of optimum welding condition was enlarged by preheating at 200°C compared with the case of RT (without preheating), and the range of NbC was hardly varied when exceeding 300°C, but on TiC it was tended to be narrower on the contrary. The beneficial effect of the preheating is considered that as the preheating temperature is increased in same welding condition, the temperature of the molten metal is increased and the fusion time is prolonged so that the carbide is well wetted to the molten base metal.

3.1.2 Shape of bead cross-section

A cross-section of the bead was changed to be finger-shaped with the narrow bottom of the penetration as the powder feeding rate was increased as shown in **Fig. 3**. These changes in the shape of bead cross-section became more remarkable as the preheating temperature and welding current were increased. It is considered that when the powder feeding rate increases the plasma arc colum is restricted and cooled by the ambient carbide powder and the colum is squeezed by the thermal pinch effect, which causes the finger-shaped penetration by increasing the plasma temperature and plasma stream. As shown in **Fig. 4**, the distribution of carbide particles on the cross-section of the bead was almost uniform except for the surface and bottom

parts. As found therein, the surface of welding metal was covered with aluminum alloy. For this reason, it can be assumed that the surface of molten pool is dented deeper during overlay welding and the bead is formed in feeding the carbide into this dent, in which case the flow of a newly melted aluminum alloy covers onto the surface of the bead according to the difference of specific gravities between aluminum and carbide. At the bottom of the finger-shaped penetration a part of low distribution density of carbide was also found. The penetration ratio (=cross-section area of the penetration/cross-section area of the bead)$\times 100$ was increased as the preheating temperature and welding current were increased but decreased as the powder feeding rate was increased. The penetration ratio exceeded 50% in both cases.

3.1.3 Carbide area ratio

The area ratio of carbide (C_p) dispersed in a overlaid metal was measured by the point counting method from a microstructure (magnification: $\times 100$) near the surface of overlaid metal by excluding reinforcement metal. The mean value of C_p measured at different three points was utilized.

Figure 5 shows the relation between C_p and carbide area ratio calculated from the powder feeding rate $[C_F = $ (powder feeding rate/cross-section area of the bead $\times$ welding speed) $\times 100]$. C_p showed a value about 1–1.5 times as large as C_F. The reason why C_p is higher is considered to be due to the existance of the part of lower distribution density of the carbide in overlaid metal at the surface and the bottom of overlaid metal as shown in Fig. 4.
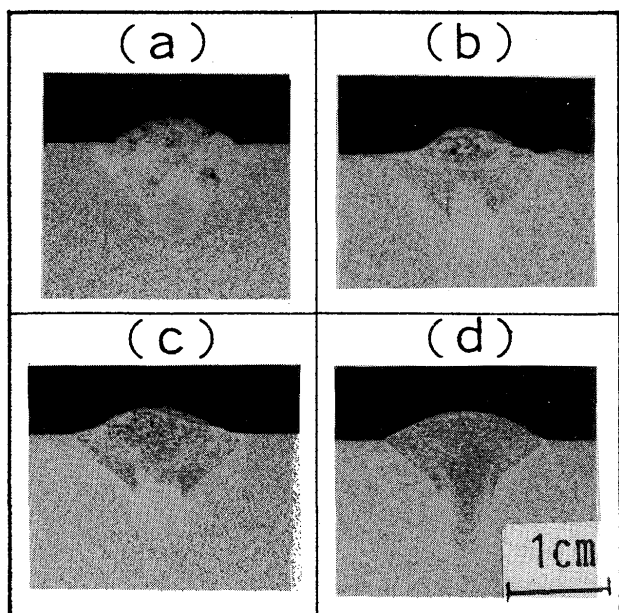

Fig. 3 Shape of bead cross-section in ralation to powder feeding rate. (a) 2.5, (b) 3.8, (c) 5.1, (d) 7.1 (cc/min); Powder: NbC, preheating temperature: 200°C, Welding current: 200A.
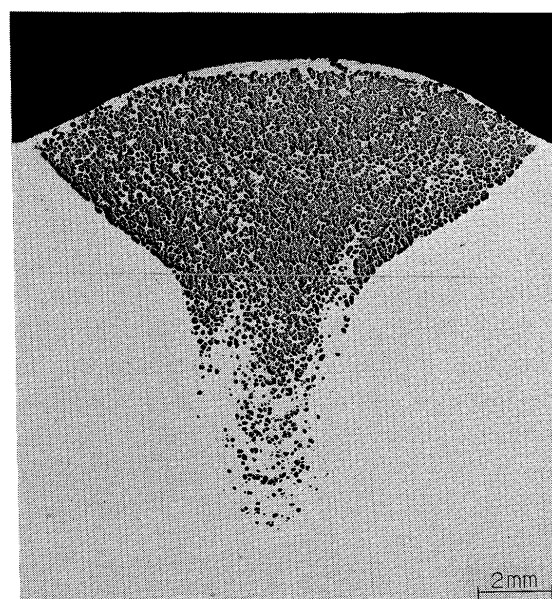

Fig. 4 Distribution of carbide (TiC) on bead cross-section at preheating temperature 200°C, welding current 200A and powder feeding rate, 7.1 cc/min.
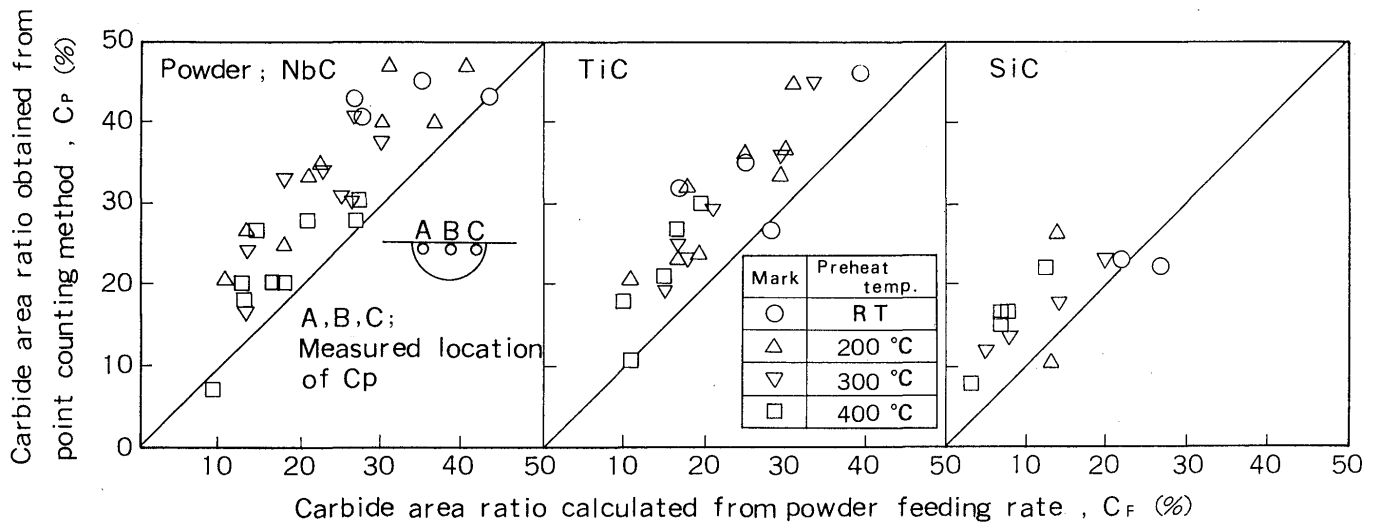
Fig. 5   Relation between carbide area ratio obtained from point counting method and carbide area ratio calculated from powder feeding rate.

C_p was tended to increase as the preheating temperature was decreased and the powder feeding rate was increased, but decreased as the welding current was increased.

3.1.4 *Effect of welding condition on occurrence of porositiy*

Porosities on overlaid metal were frequently occurred as shown in **Fig. 6**, many of which were found particularly in the vicinity of the surface of overlaid metal. **Figure 7** shows the relation between the number of porosities occurred per 1 mm^2 on the cross-section of the bead and the powder feeding rate at different preheating temperature. Without adding carbide, the porosities were not found, while in the case of adding carbide many porosities were found. Meanwhile, the porosities were tended to be reduced as powder feeding rate was increased, and the porosities were scarcely found on each carbide when the powder feeding rate reached 5.1 cc/min and more. This occurrence of porosities is considered to be caused mainly by the hydrogen of which source is the water adsorbed to the carbide particles because the porosities on aluminum alloy could be occurred mainly by the hydrogen[7-8]. It is assumed, however, that the decrease of porosities as the increase of powder feeding rate was due to the strong agitation in the molten pool caused by the thermal pinch effect of plasma arc, which promotes the release of blow hole out of the molten pool surface. Meanwhile, the cause of occurrence of porosities shall be studied further.

3.1.5 *Selection of optimum welding condition*

Figure 8 shows the ranges of optimum welding conditions for each carbide, where the appearance of the bead is good and the number of porosities per 1 mm^2
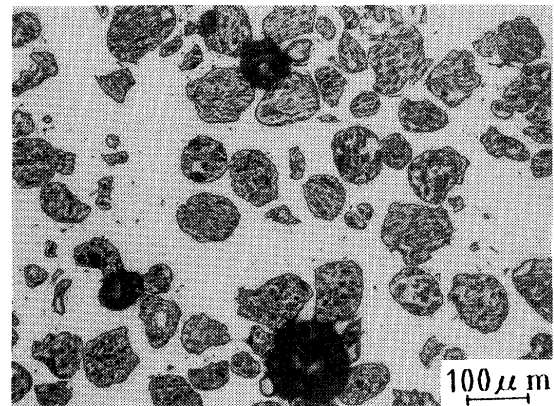

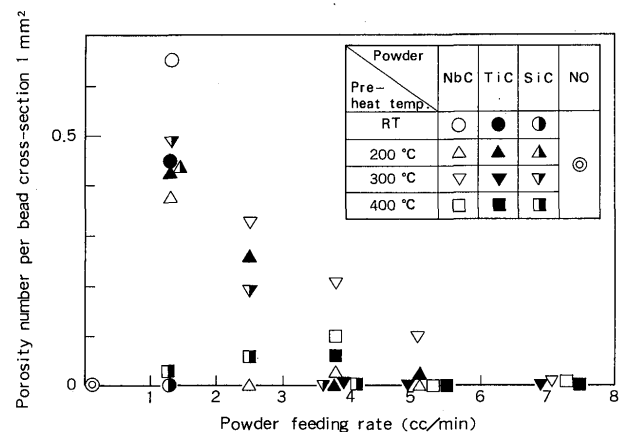**Fig. 6**   Porosities occurred in overlaid metal.

Fig. 7   Relation between porosity occurred in bead cross-section and welding conditions.

on a cross-section of the bead is less than 0.1. The range of optimum welding condition of NbC was the widest, that of TiC followed and that of SiC was remarkably narrow compared with the former two. Since the occurrence of porosity was not affected by the

type of carbide, the selected condition showed the same tendency as that of the range of the optimum welding condition, where the good appearance of bead of each carbide was obtained as shown in Fig. 2. In case of NbC and TiC at the preheating temperature of 200–300°C, the range of optimum welding condition was enlarged. In preheating at 400°C, NbC was tended to be enlarged further, while on TiC the range became narrower on the contrary. With regard to the carbide area ratio C_p in the range of optimum welding condition, C_p for NbC and TiC was about 40% in the pre-

heating condition at RT—200°C and 20–30% at 300–400°C, but it was 14–25%, for SiC slightly lower compared with the above cases.

3.2 Characteristics of overlaid metals

3.2.1 *Microstructure*

Microstructure of the cross-sections of single layer overlaid metals are shown in **Fig. 9**. Each carbide was dispersed into the matrix of aluminum alloy without melting. The distribution of NbC and TiC particles was highly dense and uniform. On the contrary,
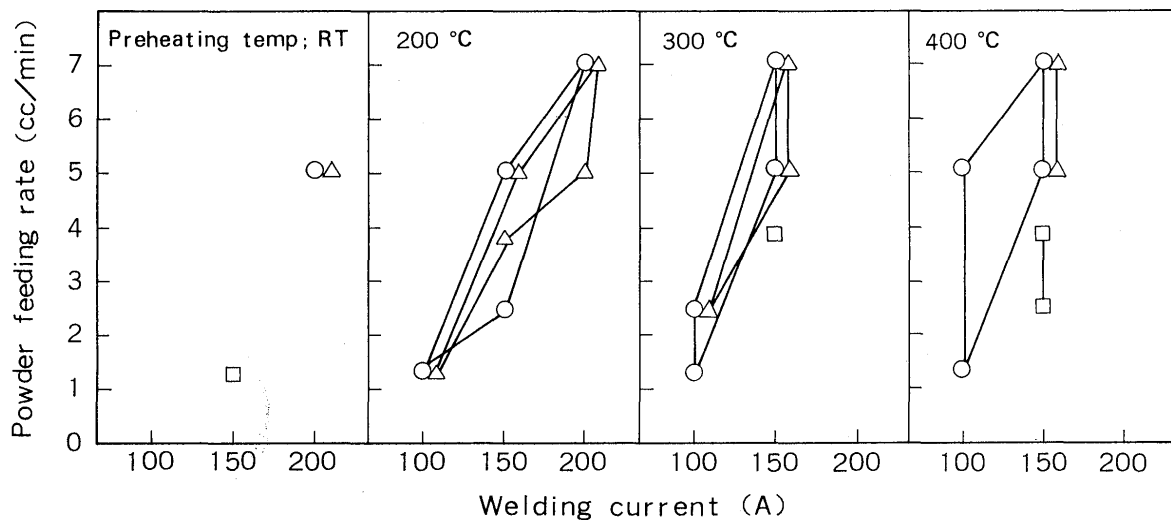

Fig. 8 Comparison of optimum welding condition ranges for NbC (○), TiC (△) and SiC (□).
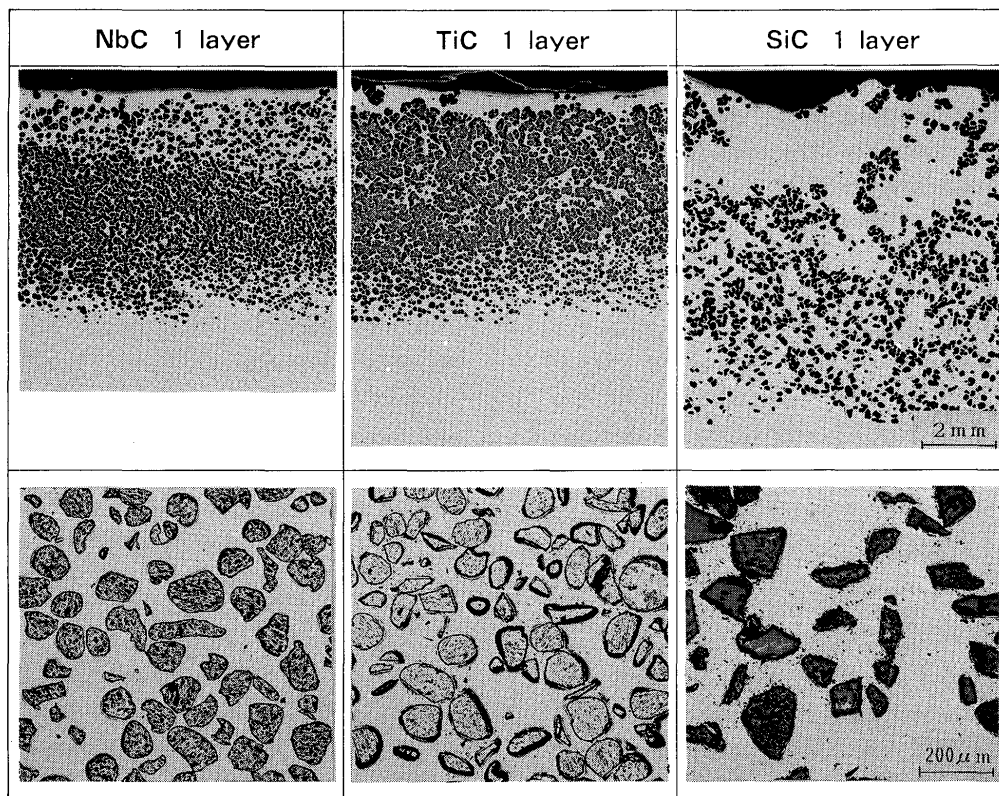

Fig. 9 Microstructure of overlaid metal (1 layer).

85

Table 2 Properties of overlaid metal

Base metal	Powder	Layer	Thickness of overlaid metal (mm)	Carbide area ratio Cp (%)	Hardness of overlaid metal (Hv 49N Load)
5083	NbC	1	5	40	141
		2	10	42	136
	TiC	1	5	39	136
		2	12	40	131
	SiC	1	· 5	28	111
		2	8	35	120

Hardness of base metal (5083) : Hv 82

the dispersion density of SiC particle was low and not uniform. It can be assumed that as the specific gravity of SiC is low, the powder is easily scattered out of the molten pool, and this causes the low C_p. On a double layer, the dispersion density of each carbide was high and uniform. Fusion boundaries between the overlaid metal and aluminum alloy were sound in all cases. An upper layer of the overlaid metal was covered with aluminum alloy and this layer became thicker in case of the double layer.

The thickness and carbide area of each overlaid metal are listed in **Table 2**. With regard to the carbide area ratio in the case of NbC and TiC they hardly changed on both single and double layers, while for SiC it was increased on double layer.

3.2.2 Hardness

Hardness of the overlaid metal is also shown in Table 2. The hardness is increased by Hv 30–50 compared with that of the aluminum alloy base metal. The hardness of a single layer remains nearly unchanged compared with that of double layer.

3.2.3 Wear resistance

Wear resistance of each overlaid metal is shown in **Fig. 10**. At the low sliding speed, the wear resistance of carbide overlaid metal showed almost no change compared with aluminum alloy base metal. When the sliding speed was increased, however, the wear resistance of carbide overlaid metal was improved remarkably compared with aluminum alloy of which wear rate was much increased. As the sliding speed is increased, the temperature of the wearing surface is raised and this causes the severe adhesion between the aluminum alloy and objective metal, S45C steel, and the adhered aluminum alloy is easely separated by a counter disk. As for the carbide overlaid metal, it is considered that the adhesion is hindered by the carbide particles dispersed in the matrix. Observing SEM image of the worn trace, in the case of aluminum alloy
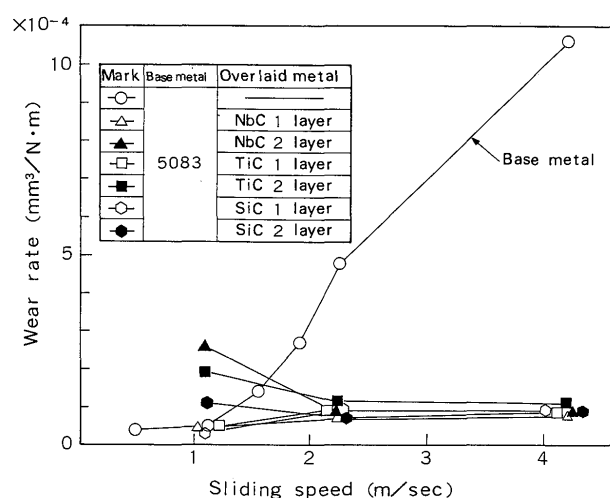

Mark	Base metal	Overlaid metal
–O–		
–△–		NbC 1 layer
–▲–		NbC 2 layer
–□–	5083	TiC 1 layer
–■–		TiC 2 layer
–◇–		SiC 1 layer
–●–		SiC 2 layer

Fig. 10 Wear property of overlaid metal. Counter disk: S45C, test temperature: RT, final load: 207.27N, sliding distance: 100 m.

base metal some traces torn off by the adhesion to a counter disk were found on the worn trace as the sliding speed was increased, while remarkable torn traces were not found on the carbide overlaid metal when the sliding speed was increased.

3.2.4 Peeling resistance

A side bending test was carried out setting the cross-section of overlaid part to be a bending surface. Less deformability of the carbide overlaid metal was found because of the occurrence of cracks in it, however no peeling from the base metal was observed. These results mean that the peeling resistance of overlaid metal from base metal is acceptable.

4. Conclusion

In order to make the carbide (NbC, TiC and SiC) dispersed aluminum matrix composite on the surface of aluminum alloy by using the plasma transferred arc welding process, the range of the optimum welding condition and various characteristics of carbide overlaid

metal were investigated. The results obtained are summerized as follows:

(1) A range of optimum welding condition providing the good appearance of the bead and less porosities was decided for each carbide. The range for NbC was the widest and for TiC it was comparably wide but for SiC it was very narrow compared with the former two.

(2) As preheating temperature and welding current became high, the cross-section of the bead showed a finger-shaped penetration due to the thermal pinch effect of plasma arc. It was found that a thin layer of aluminum alloy was formed on the surface of the bead. The bead penetration rates were exceeding 50% for each condition.

(3) The overlaid metal showed a structure containing unmolten carbide particles dispersed in the matrix of aluminum alloy. The carbide area ratio obtained in the bead reached about 40% for NbC and TiC and 28–35% for SiC in the range of optimum welding condition.

(4) The carbide area ratio in the bead was tended to increase as the increase of the powder deeding rate and the decrease of the preheating temperature and the welding current.

(5) Microscopic porosities were often appeared in the overlaid metal and tended to decrease as the increase of powder feeding rate.

(6) The hardness of carbide dispersed overlaid metal showed higher hardness of Hv 130–140 for NbC and TiC and Hv 110–120 for SiC than the base metal hardness of Hv 82.

(7) The wear resistance of carbide dispersed overlaid metal at a lower sliding speed remained nearly unchanged compared with that of the aluminum alloy base metal. At a higher speed, however, it was remarkably improved compared with that of the aluminum alloy.

(8) Through a bending test of the overlaid metal, no peeling from base metal was observed.

References

1) V.R. Ryabov, D.M. Rabkin, A.N. Muraveinik, A.N. Shalai, G.N. Voloshin, A.D. Stretovich and V.N. Bernadskii: Avt. Svarka, No 8, (1982), 20.
2) H. Grimm and J. Ruge: Z. Werkstofftech, 8 (1977), 389.
3) Dr. mont. Walther Hiller, Puchheim bei Munchen, BRD: Maschine Electrotch, 32 (1977), 2.
4) J.H.P.C. Megaw, A.S. Bransden, D.N.H. Trafford and Y. Bell: 3rd International Colloquium on Welding and Melting by Electrons and Laser Beam (1983), 269.
5) B. Vinet and S. Paidassi: Rapidly Solidified Crystal Alloys, (1985), 291.
6) K. Sakuma and T. Nishizawa: Bulletin of JIM, 10 (1971), 280 (in Japanese).
7) K. Ando and M. Fujimura: J. JWS, 32 (1963), 91 (in Japanese).
8) I. Masumoto and T. Shinoda: J. JWS, 41 (1972), 354 (in Japanese).